Journal of proteome research

Article

pubs.acs.org/jpr

Quantitative Proteomics Analysis Reveals That the Nuclear Cap-Binding Complex Proteins *Arabidopsis* CBP20 and CBP80 Modulate the Salt Stress Response

Xiangxiang Kong,[†,‡,§,∥] Lan Ma,[†,‡,§,∥] Liming Yang,[⊥] Qian Chen,[†,‡,§] Nan Xiang,[†,‡,§] Yongping Yang,[†,‡,§,⊥] and Xiangyang Hu*[,†,‡,§,⊥]

[†]Key Laboratory for Plant Diversity and Biogeography of East Asia, [‡]Plant Germplasm and Genomics Center, the Germplasm Bank of Wild Species, and [§]Institute of Tibetan Plateau Research at Kunming, Kunming Institute of Botany, Chinese Academy of Science, No. 132 Lanhei Road, Heilongtan, Kunming 650204, China

[∥]University of the Chinese Academy of Sciences, 19A Yuquanlu, Beijing 100049, China

[⊥]School of Life Sciences, Jiangsu Key Laboratory for Eco-Agriculture Biotechnology around Hongze Lake, Huaiyin Normal University, 111 Changjiang West Road, Huai'an 223300, China

Supporting Information

ABSTRACT: The cap-binding proteins CBP20 and CBP80 have well-established roles in RNA metabolism and plant growth and development. Although these proteins are thought to be involved in the plant's response to environmental stress, their functions in this process are unclear. Here we demonstrated that *Arabidopsis cbp20* and *cbp80* null mutants had abnormal leaves and flowers and exhibited increased sensitivity to salt stress. The aberrant phenotypes were more pronounced in the *cbp20/80* double mutant. Quantification by iTRAQ (isobaric tags for relative and absolute quantification) identified 77 differentially expressed proteins in the *cbp20* and *cbp80* lines compared with the wild-type Col-0 under salt stress conditions. Most of these differentially expressed proteins were synergistically expressed in *cbp20* and *cbp80*, suggesting that CBP20 and CBP80 have synergistic roles during the salt stress response. Biochemical analysis demonstrated that CBP20 and CBP80 physically interacted with each other. Further analysis revealed that CBP20/80 regulated the splicing of genes involved in proline and sugar metabolism and that the epigenetic and post-translational modifications of these genes were involved in salt stress tolerance. Our data suggest a link between CBP20/80-dependent protein ubiquitination/sumoylation and the salt stress response.

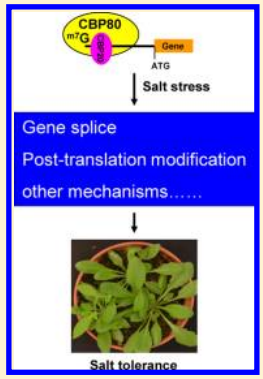

KEYWORDS: *Arabidopsis, CBP20, CBP80, iTRAQ*

INTRODUCTION

The cap-binding protein complex (CBC), which binds to the 5′ caps of transcripts generated by RNA polymerase II (PolII), plays important roles in mRNA biogenesis. It facilitates splicing and nuclear export, promotes 3′-end formation by stabilizing the interaction between mRNA and the 3′-end processing machinery, and protects mRNA transcripts from nuclease degradation.[1−3] The 5′N7-methyl guanosine cap structure is added cotranscriptionally to the 5′ end of nascent pre-mRNA molecules when they reach a length of 22−25 nucleotides and emerge from the RNA exit channel of RNA PolII. The cap is linked to the first nucleotide of the nascent transcript by an inverted 5′-5′-triphosphate bridge. Capping enzymes are recruited to the 5′ end of nascent transcripts through an interaction with the C-terminal domain (CTD) of the large subunit of PolII. This interaction is activated by the phosphorylation of Ser5 in the CTD YSPTSPS heptad repeat by the core transcriptional factor IIH (TFIIH) subunit cyclin-dependent kinase 7 (CDK7). The 5′N7-methyl guanosine cap structure can be further modified by cap-specific 2′-O RNA methytransferases in the nucleus and cytoplasm, which add a methyl group to the ribose 2-hydroxyl positions of the first and second nucleotides, giving rise to m7-GpppNm (cap 1) and m7-GpppNmN m (cap 2), respectively. In *Arabidopsis*, the nuclear CBC is composed of two subunits, AtCBP80 (80 kDa) and AtCBP20 (20 kDa). AtCBP20 has a long C-terminal tail that is rich in arginine, glycine, and aspartate, whereas AtCBP80 contains an MIF4G domain at its N terminus. The MIF4G domain is conserved in all CBP80s characterized to date, is present in eIF4G (a translation initiation factor) and NMD2 (which participates in nonsense-mediated decay (NMD)), and is thought to be involved in specific protein−protein and protein−RNA interactions. The nuclear CBC is thought to be involved in pre-mRNA alternative splicing and microRNA biogenesis and to regulate multiple physiological aspects of growth, development, and environmental stress responses.[2−5] Recently, the nuclear CBC was shown to function in the drought stress response.[5] However, the functions of the nuclear CBC in environmental stress responses other than the drought

Received: December 18, 2013
Published: April 1, 2014

dx.doi.org/10.1021/pr4012624 | *J. Proteome Res.* 2014, 13, 2495−2510

stress response and the underlying mechanisms remain to be determined.

Plants have evolved mechanisms that allow them to withstand stressful environments. Salt stress is an environmental stress that severely limits crop yield.[6] Knowledge of the mechanisms that underlie the salt stress response could be used to engineer plants with improved resistance to salt stress. Upon exposure to salt stress, plants attempt to reestablish ionic and osmotic homeostasis, detoxify reactive oxygen species, and adjust cell division and expansion to a level suitable for the particular conditions.[2] Transcriptomic changes and alternative splicing of mRNA play central roles in modulating the plant's physiological response to stress.[2,6−8] In addition, epigenetic regulation (e.g., DNA methylation and histone modifications) is crucial during the stress response.[9] Furthermore, posttranscriptional modification (e.g., proteosome-dependent ubiquitination and sumoylation) controls the plant's response to environmental stress by altering the stability of target proteins.[10] Given that various regulatory mechanisms are involved in the plant adaptation to saline stress, the identification of isolated transcriptomic changes do not provide a comprehensive understanding of this process, and more attention to the change at the post-transcriptional or post-translational level is also necessary. Comparative proteomics approaches that investigate molecular responses to environmental stress at the posttranscriptional or epigenetic level have been proven to be far more informative.[11,12]

To understand the regulatory functions of CBP20 during the plant's response to salt stress, particularly beyond the transcriptional level, we adopted a comparative quantitative proteomics approach. We sought to identify differences in protein expression among *cap20* and *cbp80* null mutants and wild-type *Arabidopsis* during the salt stress response. We found that the mutant and control plants exhibited striking differences in the expression of protein kinases and of proteins associated with ion flux, oxidative stress, redox status, DNA and chromatin architecture, and mRNA splicing under salt-stress conditions and also in proteins linked to metabolic changes, including those involved in proline and sugar metabolism. Furthermore, we found that CBP20 synergistically enhanced the effect of CBP80 during the salt stress response in *Arabidopsis*. These results indicate that nuclear CBC-mediated posttranscriptional and epigenetic modification have important roles during the salt stress response and suggest a novel strategy for engineering crops with improved salt stress tolerance.

MATERIALS AND METHODS

Plant Growth and Treatment

Arabidopsis thaliana ecotype (Col-0) plants were grown on Murashige and Skoog (MS) plates at 22 ± 2 °C under 16 h light (100 μmol $m^{-2}s^{-1}$)/8 h dark conditions. The T-DNA insertion mutants *cbp20* (*Salk-086644*) and *cbp80* (*Salk-24285*) were obtained from ABRC (www.arabidopsis.org), verified using the primers listed in Supplemental Table 1 in the Supporting Information, and grown as previously described. For salt stress treatment, wild-type Col-0, *cbp20*, *cbp80*, and *cbp20/80* double mutant seeds were sown on MS medium containing various concentrations of sodium chloride (25, 75, and 100 mM NaCl, respectively). After 1 week of growth, photographs were taken and root lengths were measured. For salt stress treatment in soil, the culture soil was prepared by mixing fertilizer, vermiculite, and perlite at a ratio of 3:1:1. Seedlings were first grown on MS medium for 2 weeks and then transferred to the prepared soil for growth under the same conditions as previously described. After 1 week of growth, the soil was irrigated with 100 mM NaCl solution once every other day. After 2 weeks of treatment, the plants were photographed and biomass was measured.

Proline, Sugar, and Starch Content Measurements

Proline and starch content were measured as described.[17,18] In brief, the treated seedlings were harvested, weighed, and extracted in 3% sulfosalicylic acid. An aliquot of each extract (2 mL) was incubated with 2 mL of ninhydrin reagent (2.5% [w/v] ninhydrin, 60% [v/v] glacial acetic acid, and 40% 6 M phosphoric acid) and 2 mL of glacial acetic acid at 100 °C for 40 min, and the reaction was terminated in an ice bath for 15 min. Toluene (5 mL) was added, followed by vortexing and incubation at 23 °C for 24 h. The absorbance was measured at 520 nm. Treated seedlings (1 g) were used to measure soluble sugar content using a Sugar Assay Kit, according to the manufacturer's protocol (Sigma-Aldrich). After grinding the plants in liquid nitrogen, soluble sugars were extracted two times with 80% ethanol, and fractions were collected and centrifuged at 12 000 g for 10 min. Ethanol was evaporated from the supernatant using a vacuum evaporator, and the volume of the solution was adjusted to 400 mL using triple-distilled water to measure the sugar content. The insoluble pellets were used to measure the starch content using the Starch Assay Kit, according to the manufacturer's protocol (Megazyme). The starch content in the leaves was also indicated by iodine staining using the Lugol solution (containing aqueous potassium iodide plus iodine, cat. L6146, Sigma Chemical).

Protein Extraction

After 3 days of growth on MS plates containing 100 mM NaCl, the seedlings were collected by liquid nitrogen freezing and proteins were extracted using a previously described phenol extraction procedure.[13] In brief, ∼1 g of frozen seedlings was ground with a mortar in liquid nitrogen and 5 mL of extraction buffer containing 100 mM Tris−HCl pH 7.8, 100 mM KCl, 50 mM L-ascorbic acid, 1% (v/v) Triton X-100, 1% (v/v) β-mercaptoethanol, and 1 mM phenylmethylsulfonyl fluoride (PMSF) was added. After centrifugation (12 000*g*; 15 min; 4 °C), the resulting suspension solution was transferred to a 20 mL tube, and Tris-phenol (2 volus; pH 8.0, Amersco, Canada) was added. The mixture was thoroughly vortexed before centrifuging at 12 000*g* for 15 min at 4 °C. The upper phenolic phases were transferred to a 50 mL tube, and then 5 volumes of 100 mM ammonium acetate/methanol were added. After careful mixing, the mixture was stored at −20 °C overnight. The supernatant was removed carefully after centrifugation at 13 000*g* for 15 min at 4 °C, and the protein pellets were used immediately or suspended in 25 mL of ice-cooled methanol for 2 h at −20 °C for further analysis.

Protein Digestion, iTRAQ Labeling, and Protein Quantification

After three independent treatments, the seedlings were pooled to yield one biological replicate. Four biological replicates, each containing 75 mg protein, were prepared for iTRAQ labeling. Detailed information about sample labeling is provided in Supplemental Table 2 in the Supporting Information. The pellet protein was dissolved in 1% SDS, 100 mM triethylammonium bicarbonate, pH 8.5, followed by reduction,

alkylation, trypsin digestion, and labeling using 8-plex iTRAQ reagent kits, according to the manufacturer's instructions (AB Sciex, USA). Six groups of replicate sample, consisting of three groups of sample (i.e., col-0, *cbp20*, and *cbp80*) before saline treatment and three groups of sample (i.e., *cbol-0*, *cbp20*, and *cbp80*) after saline treatment were used, and every replicate group consisted of three samples. Thus, at least 18 samples were required for labeling. Information about sample labeling is provided in Supplemental Table 2 in the Supporting Information. After labeling, the samples were combined and lyophilized, and the peptide mixture was dissolved in strong cation exchange (SCX) solvent A (25% v/v acetonitrile, 10 mM ammonium formate, pH 2.8). The peptides were fractionated on an Agilent HPLC system 1100 with a polysulfethyl A column (2.1 × 100 mm, 5 μm, 300 A, PolyLC, Columbia, MD). Peptides were eluted at a flow rate of 200 μL/min with a linear gradient of 0−20% solvent B (25% v/v acetonitrile, 500 mM ammonium formate) over 50 min, followed by ramping up to 100% solvent B in 5 min and holding for 10 min. The absorbance at 214 nm was monitored, and a total of 12 fractions were collected. Each SCX fraction was lyophilized and dissolved in solvent A (3% acetonitrile v/v, 0.1% formic acid v/v) and then was submitted to analyze with a Q-Exactive Hybrid Quadrupole-Orbitrap mass spectrometer (Thermo Finnigan Scientific, San Jose, CA). Samples were separated on Hypersile Gold C18 column (100 mm × 2.1 mm, 1.9 μm) (Thermo Fisher Scientific, Pittsburgh, PA). Peptides were eluted with a linear gradient of acetonitrile/0.1% formic acid from 3 to 50% in 90 min at a flow rate of 250 nL/min. Peptides were then sprayed into the orifice of the Q-Exactive MS/MS system with a spray voltage of 2.2 kV. Full-scan mass spectra were performed over 200−1800 m/z at high resolution at 60 000. At least the four most intense precursor ions were selected for collision-induced fragmentation in the linear ion trap with 50−2000 m/z and 30−2000 ms at a resolution of 7500. Dynamic exclusion was employed within 40 s to prevent repetitive.

The raw LC−MS/MS files were analyzed using Proteome Discoverer 1.3 (Thermo Fisher Scientific, Pittsburgh, PA). The software was connected to the Mascot Search Engine server, version 2.3 (Matrix Science, Boston, MA). The spectra were searched against an *A. thaliana* database downloaded from TAIR10 version (TAIR10_pep_20110103_representative_gene_model) available at ftp://ftp.arabidopsis.org/Sequences/blast_datasets/OLD/ dated April 2012 with a total of 59 687 entries including 1413 small proteins and 45 common contaminants. Search parameters included iTRAQ 8-plex quantification, carbamidomethylation of cysteine was set as a fixed modification, and oxidation of methionine was set as a variable modification. Trypsin was specified as the proteolytic enzyme, and one missed cleavage was allowed. Peptide mass tolerance was set at10 ppm; fragment mass tolerance was set at 0.1 Da. An automatic decoy database search was performed as part of the search. False discovery rates (FDRs) for peptide identification of all searches were <1.0%. The data were prefiltered to exclude MS/MS spectra containing fewer than three peaks or with a total ion count below 50. Mascot results were filtered with the Mascot Percolator package to improve the accuracy and sensitivity of peptide identification. For differential analyses, all proteins identified and quantified with at least four independent peptides with a high degree of confidence (FDR 1%) were selected. The quantification was performed normalizing the results of all of the measured iTRAQ reported ratios value by Proteome Discoverer1.3 software. Only the significant ratios from the replicates were used to calculate the average ratio for the protein. It should be noted that each p value was generated based on quantitative information derived from at least three independent peptides in each replicate. Cut-offs of 2- or 0.6-fold were set to indicate up-regulation or down-regulation of proteins, and a p value of <0.05 was used to indicate significance.

RNA Extraction and RT-PCR Analysis

Total RNA was extracted from the whole young seedlings subjected to different treatments using TRIzol reagent (Invitrogen) and reverse-transcribed to yield cDNA using M-MLV reverse transcriptase (Promega).[14] The alternatively spliced fragments were amplified from the cDNA using primers listed in Supplemental Table 1 in the Supporting Information. The amplification products were separated by electrophoresis on 2% agarose gels.

Immunoblot Analysis

Proteins from seedlings subjected to different treatments were extracted in 50 mM Tris pH 7.5, 150 mM NaCl, 1 mM EDTA, 0.1% Triton X-100, 0.5% β-mercaptoethanol, and 1 mM PMSF with vigorous vortexing. After centrifugation at 20 000g, 4 °C for 15 min, the supernatants were collected. The supernatant protein concentration was determined using the Bio-Rad Quick Start Bradford Kit (cat. 500-0201), according to the manufacturer's instructions (Bio-Rad Laboratories, USA). The extracted proteins (10 μg per sample) were separated on 12% SDS−PAGE gels and transferred to nitrocellulose membranes using a Mini-PROTEAN system (Bio-Rad Laboratories, USA). The membranes were blocked for 1 h at room temperature in phosphate-buffered saline (PBS) containing 5% milk and washed at least three times with PBS buffer containing 0.5% Tween 20 (PBST), each for 5 min. Primary antibodies were prepared in PBS buffer containing 1% BSA and then incubated with the membranes overnight at 4 °C. After removing unbound antibodies by washing with PBST, the blots were incubated with rabbit antirabbit IgG secondary antibody (horseradish peroxidase conjugates, Promega) in PBST buffer at a dilution of 1:10 000 and visualized using a chemiluminescent kit (Thermo Fisher Scientific, USA). The P5CS1 antibody (1:1000) was prepared by immunizing a rabbit with a synthesized peptide (MEELDRSRAFARDVK) corresponding to the N-terminal fragment of *Arabidopsis* P5CS1. Anti-SUMO (1:1000) and anti-Ubi (1:2000) antibody were purchased from Agrisera (Vannas, Sweden).

Plant Transformation and Histochemical GUS Assay

The *CBP20* and *CBP80* promoters were PCR-amplified from *Arabidopsis* genomic DNA. The CBP20 promoter fragment was cloned into a modified pEGAD-GFP vector in which GFP was replaced with GUS to generate the *ProCBP20::GUS* construct, and the CBP80 promoter fragment was cloned into the pGREEN:GUS[15] in which the GUS gene was inserted into the basic pGREEN vector to generate *ProCBP80::GUS* constructs. The primer sequences used for vector construction are listed in Supplemental Table 1 in the Supporting Information. The constructs were then transformed into Agrobacterium GV3101, and transgenic lines harboring *ProCBP2::GUS* and *ProCBP80::GUS* were obtained by floral dip and hygromycin screening.[15] GUS staining was detected as reported previously.[16]

dx.doi.org/10.1021/pr4012624 | J. Proteome Res. 2014, 13, 2495−2510

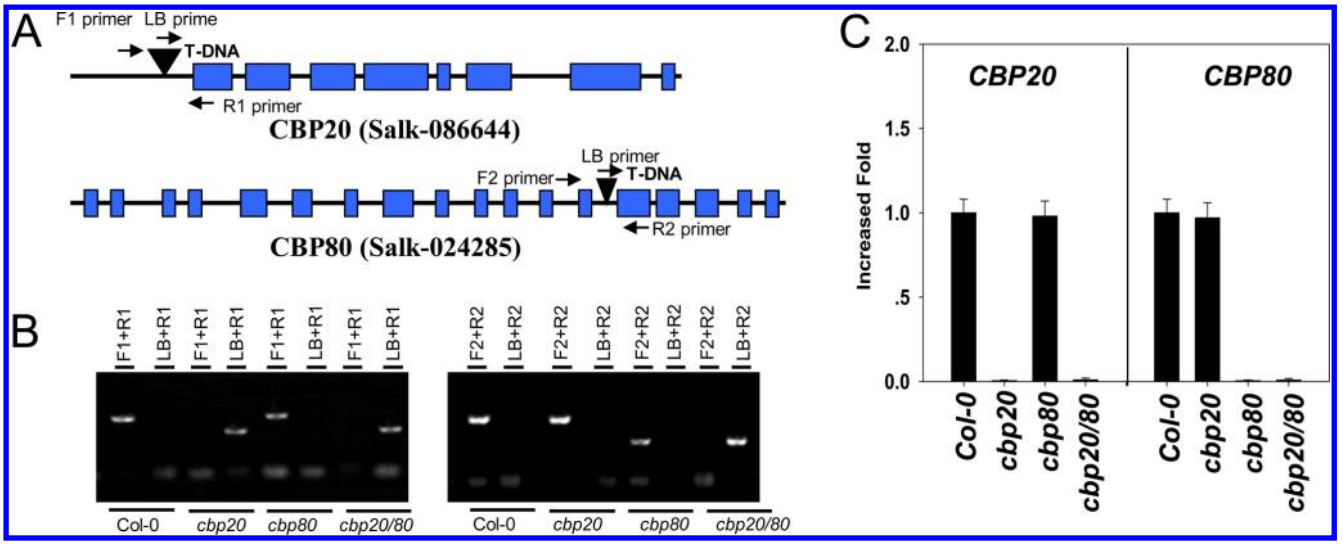

Figure 1. Verification and phenotype analysis of the *cbp20* and *cbp80* mutants. (A) Structure of *CBP20* and *CBP80* and the T-DNA insertion sites in these two genes. (B) Verification of the T-DNA insertion in *CBP20* and *CBP80* using specific primers. The primer pair F1 and R1 amplified a band from the wild-type (Col-0) line but not from *cbp20* or *cbp80*. (C) Quantitative RT-PCR analysis of *CBP20* and *CBP80* transcript in the *cbp20* or *cbp80* mutants. Bar = ±SE, $n = 3$.

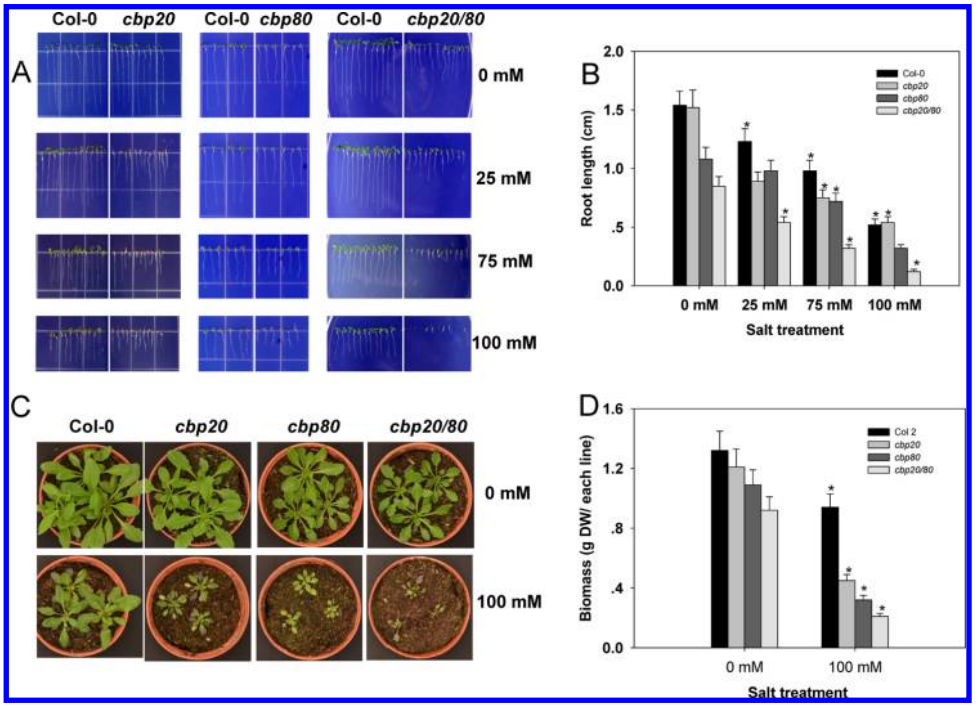

Figure 2. Sensitivity of *cbp20*, *cbp80*, and *cbp20/80* to salt stress. (A,B) Phenotype of wild-type, *cbp20*, *cbp80*, and *cbp20/80* seedlings grown on MS medium containing the indicated concentrations of NaCl. Photographs were taken and the root lengths were recorded after 2 weeks of growth. (C,D) Phenotype and biomass of wild-type, *cbp20*, *cbp80*, and *cbp20/80* seedlings grown in soil irrigated with 100 mM NaCl. Wild-type, *cbp20*, *cbp80*, and *cbp20/80* seeds were germinated and allowed to grow on normal MS medium for 1 week and were then transferred to soil irrigated with 100 mM NaCl. Seedlings were photographed after 2 weeks of growth (C) and the biomass was measured (D). Data are the means ± SD ($n = 16$), and bars labeled with an asterisk are significantly different at $p < 0.05$ compared with the control experiments (Student's t test).

RESULTS AND DISCUSSION

Aberrant Leaf and Flower Morphologies of the cbp20 and cbp80 Mutant

To establish the roles of CBP20 and CBP80, we first identified *cbp20* (*Salk-086644*) and *cbp80* (*Salk-24285*) T-DNA null mutants. As shown in Figure 1A, *CBP20* contains 8 exons and *CBP80* contains 18. The exogenous T-DNA transporter inserted into the 5'-UTR region of *CBP20* inactivated transcription in the *cbp20* mutant, and the T-DNA inserted into the 13th exon of *CBP80* inactivated transcription in the *cbp80* mutant (Figure 1A). Using primers designed to detect the T-DNA fragment (LB primer), the left region (F1, F2 primer), and the right region (R1, R2 primer) of *CBP20/CBP80*, we found that the F1/R1 and F2/R2 primer pairs successfully amplified bands in the wild-type (Col-0) lines but failed to amplify fragments in the *cbp20* and *cbp80* lines due to the T-DNA insertion. The LB/R1 and LB/R2 primer pairs

dx.doi.org/10.1021/pr4012624 | J. Proteome Res. 2014, 13, 2495−2510

Table 1. Salt-Induced Differential Proteins in col-0, *cbp20*, and *cbp80* after 100 mM Salt Stress For 3 Days Identified by iTRAQ Analysis

accession number[a]	protein names	117:113[b] / 118:114[b]	*p* value	119:115[b] / 121:116[b]	*p* value	average degree	117:113[c] / 118:114[c]	*p* value	119:115[c] / 121:116[c]	*p* value	average degree
	Energy and Material Metabolism										
AT1G12 200	flavin-containing monooxygenase	2.952	0.037	2.717	0.038	2.645	0.899	0.013	0.782	0.004	0.808
		2.565	0.023	2.346	0.035		0.864	0.005	0.687	0.005	
AT1G22 440	alcohol dehydrogenase-like 2	2.294	0.017	2.952	0.021	2.545	1.144	0.033	1.216	0.046	1.161
		2.278	0.009	2.654	0.032		1.125	0.003	1.158	0.005	
AT1G28 110	serine carboxypeptidase-like 45	0.804	0.041	0.727	0.003	0.760	2.603	0.034	2.853	0.003	2.655
		0.759	0.012	0.751	0.036		2.612	0.009	2.552	0.004	
AT1G28 290	arabinogalactan protein 31	0.805	0.006	0.983	0.016	0.879	2.905	0.001	2.616	0.042	2.769
		0.845	0.009	0.882	0.009		2.895	0.005	2.658	0.035	
AT1G31 220	phosphoribosylglycinamide formyltransferase	0.529	0.023	0.554	0.042	0.565	1.306	0.049	1.251	0.004	1.276
		0.652	0.008	0.525	0.032		1.323	0.006	1.225	0.004	
AT1G32 550	ferredoxin	2.778	0.049	2.632	0.015	2.600	1.115	0.020	1.170	0.023	1.185
		2.754	0.024	2.236	0.039		1.210	0.005	1.246	0.024	
AT1G54 630	acyl carrier protein 3, chloroplastic	0.958	0.046	0.866	0.026	0.885	1.798	0.021	1.748	0.021	1.787
		0.857	0.041	0.858	0.021		1.854	0.021	1.746	0.035	
AT1G66 280	beta-glucosidase 22	0.855	0.030	0.706	0.021	0.770	1.545	0.002	1.639	0.036	1.600
		0.793	0.032	0.724	0.032		1.556	0.008	1.660	0.039	
AT2G28 520	vacuolar proton ATPase	2.550	0.035	2.833	0.034	2.522	1.201	0.021	1.097	0.012	1.158
		2.458	0.031	2.245	0.031		1.220	0.005	1.112	0.035	
AT5G61 290	flavin-binding monooxygenase family protein	2.896	0.047	2.968	0.005	2.741	1.556	0.009	1.521	0.008	1.532
		2.659	0.045	2.441	0.006		1.526	0.007	1.524	0.007	
AT4G14 240	cystathionine beta-synthase	1.516	0.020	1.518	0.036	1.589	2.976	0.034	2.938	0.030	2.918
		1.458	0.023	1.865	0.035		2.859	0.007	2.899	0.058	
AT4G15 210	cytosolic beta-amylase	2.898	0.016	2.806	0.042	2.598	0.744	0.029	0.952	0.016	0.835
		2.569	0.011	2.120	0.021		0.775	0.024	0.868	0.005	
AT4G31 140	*O*-glycosyl hydrolases family 17 protein	2.781	0.017	2.782	0.043	2.646	1.133	0.027	1.182	0.009	1.142
		2.268	0.020	2.754	0.035		1.139	0.028	1.112	0.005	
AT5G58 390	peroxidase superfamily protein	2.789	0.011	2.775	0.010	2.743	1.121	0.036	1.148	0.048	1.175
		2.747	0.020	2.660	0.021		1.220	0.036	1.210	0.021	
AT4G36 910	encodes a single cystathionine beta-synthase domain-containing protein	0.514	0.003	0.531	0.017	0.522	0.457	0.006	0.411	0.038	0.434
		0.521	0.028	0.523	0.021		0.428	0.007	0.440	0.035	
AT1G80 750	ribosomal protein L30/L7 family protein	2.759	0.039	2.691	0.019	2.590	2.828	0.036	2.898	0.022	2.859
		2.443	0.036	2.465	0.021		2.885	0.008	2.825	0.035	
AT5G46 110	encodes a chloroplast triose phosphate	3.205	0.048	3.663	0.022	3.327	3.016	0.007	3.055	0.036	3.076
		3.120	0.042	3.321	0.036		3.121	0.012	3.112	0.006	
AT4G13 010	oxidoreductase	2.986	0.001	2.837	0.030	2.637	2.722	0.033	2.716	0.005	2.756
		2.569	0.025	2.157	0.034		2.859	0.023	2.725	0.008	
AT1G09630	encodes a putative GTP-binding protein	0.218	0.044	0.224	0.035	0.225	0.304	0.013	0.369	0.029	0.335
		0.241	0.022	0.215	0.025		0.332	0.023	0.335	0.007	
AT4G10 340	photosystem II encoding the light-harvesting chlorophyll *a*/*b* binding protein	0.356	0.029	0.616	0.017	0.466	0.326	0.016	0.374	0.018	0.347
		0.323	0.025	0.569	0.025		0.359	0.045	0.329	0.024	

dx.doi.org/10.1021/pr401262d | *J. Proteome Res.* 2014, 13, 2495−2510

Table 1. continued

accession number[a]	protein names	117:113[b]	*p* value	119:115[b]	*p* value	average	117:113[c]	*p* value	119:115[c]	*p* value	average
		118:114[b]	*p* value	121:116[b]	*p* value	degree	118:114[c]	*p* value	121:116[c]	*p* value	degree
	Energy and Material Metabolism										
AT3G17 430	nucleotide/sugar transporter family protein	0.339	0.014	0.605	0.023	0.472	0.465	0.043	0.405	0.030	0.439
		0.332	0.025	0.612	0.025		0.445	0.024	0.440	0.035	
Defense Response-Related											
AT1G02920	encodes glutathione transferase	0.749	0.021	0.765	0.039	0.724	2.842	0.008	2.851	0.004	2.790
		0.598	0.030	0.782	0.025		2.585	0.012	2.882	0.007	
AT4G18 350	encodes 9-*cis*-epoxycarotenoid dioxygenase	0.430	0.045	0.456	0.019	0.462	0.496	0.028	0.419	0.000	0.451
		0.552	0.032	0.410	0.025		0.442	0.023	0.446	0.004	
AT2G39 800	encodes a delta1-pyrroline-5-carboxylate synthase	0.352	0.006	0.441	0.038	0.394	0.204	0.013	0.319	0.006	0.270
		0.336	0.012	0.446	0.024		0.221	0.024	0.335	0.002	
AT1G01470	encodes late-embryogenesis abundant protein whose mRNA levels are induced in response to wounding and light stress	0.442	0.005	0.438	0.002	0.434	0.318	0.035	0.463	0.002	0.383
		0.445	0.009	0.410	0.025		0.325	0.035	0.425	0.032	
AT3G24 170	encodes a cytosolic glutathione reductase	0.342	0.027	0.423	0.037	0.382	0.303	0.032	0.368	0.042	0.335
		0.339	0.032	0.425	0.034		0.334	0.013	0.336	0.035	
AT5G44 000	glutathione S-transferase family protein	0.526	0.047	0.501	0.020	0.537	0.448	0.045	0.422	0.033	0.435
		0.597	0.021	0.523	0.035		0.445	0.024	0.426	0.039	
AT3G13 340	transducin/WD40 repeat-like superfamily protein	0.379	0.006	0.491	0.004	0.416	0.387	0.000	0.442	0.048	0.420
		0.367	0.005	0.425	0.007		0.410	0.005	0.440	0.004	
Calcium Signal Transduction											
AT2G41 410	calcium-binding EF-hand family protein	2.343	0.025	2.488	0.023	1.895	1.972	0.015	1.826	0.047	1.885
		0.339	0.036	2.410	0.036		1.858	0.002	1.882	0.035	
AT2G33 380	calcium binding protein	0.414	0.009	0.412	0.038	0.419	0.544	0.032	0.453	0.011	0.497
		0.447	0.005	0.402	0.037		0.552	0.035	0.440	0.038	
Ubiquitin and Sumoylation Modification											
AT1G55 860	E3 ubiquitin ligase family protein	2.192	0.031	2.469	0.014	2.227	1.113	0.009	1.154	0.029	1.123
		2.121	0.021	2.125	0.024		1.112	0.005	1.112	0.035	
AT2G36 060	ubiquitin-conjugating enzyme E2 variant 1C	2.202	0.004	1.869	0.049	2.038	1.773	0.019	1.623	0.037	1.667
		2.223	0.005	1.858	0.034		1.747	0.003	1.526	0.038	
AT4G25 440	zinc finger WD40 repeat protein 1 (ZFWD1)	1.497	0.036	1.465	0.017	1.479	2.172	0.030	2.185	0.013	2.199
		1.529	0.039	1.425	0.024		2.220	0.021	2.220	0.014	
AT1G55 860	encodes a ubiquitin-protein ligase containing a HECT domain. There are six other HECT-domain UPLs in *Arabidopsis*.	3.192	0.023	3.464	0.015	3.304	3.424	0.008	3.794	0.004	3.421
		3.326	0.020	3.232	0.035		3.232	0.008	3.232	0.007	
AT4G23 940	FtsH extracellular protease family	2.154	0.007	2.159	0.049	2.165	2.173	0.026	2.359	0.004	2.244
		2.226	0.005	2.120	0.038		2.220	0.009	2.225	0.007	
AT3G47 060	encodes an FtsH protease that is localized to the chloroplast	2.174	0.042	2.159	0.022	2.171	2.224	0.032	2.341	0.021	2.255
		2.240	0.032	2.110	0.039		2.225	0.012	2.228	0.005	
AT3G48 340	cysteine proteinases superfamily protein	2.143	0.044	2.058	0.041	2.119	1.682	0.011	1.996	0.024	1.819
		2.220	0.020	2.054	0.024		1.742	0.015	1.856	0.035	
AT5G60 410	encodes a plant small ubiquitin-like modifier (SUMO) E3 ligase	0.529	0.026	0.453	0.008	0.492	0.392	0.016	0.581	0.036	0.464
		0.562	0.024	0.425	0.035		0.332	0.035	0.552	0.024	
AT5G05080	ubiquitin-conjugating enzyme 22	0.627	0.041	0.417	0.028	0.524	0.455	0.010	0.479	0.034	0.454

dx.doi.org/10.1021/pr401262d | *J. Proteome Res.* 2014, 13, 2495−2510

Table 1. continued

accession number[a]	protein names	117:113[b]	*p* value	119:115[b]	*p* value	average degree	117:113[c]	*p* value	119:115[c]	*p* value	average degree
		118:114[b]	*p* value	121:116[b]	*p* value		118:114[c]	*p* value	121:116[c]	*p* value	
	Energy and Material Metabolism										
Ubiquitin and Sumoylation Modification											
		0.625	0.002	0.426	0.034		0.440	0.001	0.442	0.007	
Epigenetics Modification											
AT1G10 930	ATP-dependent DNA helicase	3.133	0.009	3.389	0.042	3.266	1.076	0.005	1.122	0.041	1.134
		3.223	0.006	3.320	0.034		1.118	0.005	1.220	0.025	
AT3G07250	putative RNA-binding protein	0.638	0.011	0.388	0.038	0.496	0.732	0.039	0.707	0.035	0.728
		0.625	0.020	0.332	0.038		0.748	0.005	0.726	0.032	
At2g25 170	encodes an SWI/SWF nuclear-localized chromatin remodeling factor of the CHD3 group	2.185	0.001	2.084	0.029	2.131	1.145	0.048	1.124	0.003	1.146
		2.220	0.020	2.035	0.031		1.202	0.035	1.112	0.004	
At2g47 110	polyubiquitin gene	2.496	0.003	1.783	0.025	2.147	1.332	0.036	1.345	0.036	1.345
		2.658	0.009	1.652	0.015		1.339	0.025	1.363	0.008	
AT3G54 610	encodes a histone acetyltransferase	2.048	0.018	2.383	0.005	2.244	2.826	0.042	2.702	0.037	2.064
		2.226	0.015	2.320	0.009			0.014	2.726	0.032	
AT4G25 500	encodes an arginine/serine-rich splicing factor	0.557	0.029	0.388	0.048	0.457	0.206	0.033	0.275	0.008	0.241
		0.559	0.036	0.325	0.024		0.225	0.039	0.256	0.004	
AT1T74 560	bind histones Histone2A and Histone2B and associate with chromatin in vivo	0.238	0.041	0.310	0.043	0.306	0.403	0.044	0.426	0.033	0.424
		0.321	0.015	0.356	0.031		0.421	0.024	0.446	0.021	
AT3G26 560	ATP-dependent RNA helicase	0.284	0.019	0.369	0.028	0.332	0.258	0.022	0.311	0.001	0.282
		0.330	0.036	0.345	0.032		0.224	0.035	0.335	0.004	
AT5G03740	H2-type histone eactylase HDAC	0.265	0.015	0.366	0.026	0.310	0.373	0.024	0.334	0.005	0.282
		0.298	0.032	0.310	0.021		0.332	0.038	0.328	0.007	
AT5G59 910	HTB4 for DNA binding	2.198	0.038	2.362	0.026	2.277	2.285	0.022	2.128	0.046	2.215
		2.225	0.036	2.321	0.012		2.225	0.035	2.220	0.021	
Protein Kinase and Phosphatase											
AT1G60 490	phosphatidylinositol 3-kinase	1.185	0.047	1.147	0.043	1.144	2.065	0.002	2.356	0.008	2.216
		1.120	0.015	1.125	0.024		2.220	0.038	2.224	0.007	
AT1G49 820	methylthioribose kinase	1.118	0.038	0.978	0.037	1.062	2.212	0.014	2.054	0.029	2.124
		1.226	0.035	0.925	0.031		2.128	0.023	2.102	0.032	
AT1G78 090	trehalose-phosphate phosphatase B	0.919	0.035	0.904	0.022	0.909	0.445	0.024	0.409	0.030	0.431
		0.902	0.039	0.910	0.021		0.428	0.039	0.442	0.002	
AT2G27 970	CDK-subunit 2 (CKS2)	2.124	0.044	2.106	0.042	2.140	1.708	0.004	1.723	0.035	1.720
		2.226	0.036	2.105	0.035		1.725	0.037	1.724	0.007	
AT2G17 700	CT-like protein tyrosine kinase family protein	2.223	0.014	2.603	0.001	2.287	2.244	0.034	2.637	0.034	2.381
		2.019	0.023	2.301	0.005		2.220	0.035	2.422	0.024	
Cell Division and Structure											
AT1G20 610	CycB2.3	0.349	0.014	0.452	0.037	0.388	0.843	0.008	0.849	0.023	0.817
		0.326	0.021	0.425	0.031		0.782	0.009	0.795	0.021	
AT1G20 190	alpha-expansin11	0.474	0.012	0.455	0.008	0.404	0.831	0.050	0.705	0.028	0.798
		0.268	0.036	0.420	0.009		0.886	0.021	0.771	0.008	
AT1G65 681	beta-expansin6	0.752	0.004	0.749	0.035	0.738	0.403	0.035	0.382	0.020	0.389

dx.doi.org/10.1021/pr401262d | J. Proteome Res. 2014, 13, 2495−2510

Table 1. continued

accession number[a]	protein names	117:113[b]	*p* value	119:115[b]	*p* value	average	117:113[c]	*p* value	119:115[c]	*p* value	average
		118:114[b]	*p* value	121:116[b]	*p* value	degree	118:114[c]	*p* value	121:116[c]	*p* value	degree
	Energy and Material Metabolism										
Cell Division and Structure											
		0.725	0.005	0.725	0.035		0.442	0.037	0.329	0.032	
AT1G47 210	CYCA3.2	0.894	0.046	0.836	0.031	0.721	0.265	0.016	0.385	0.048	0.309
		0.326	0.036	0.826	0.036		0.246	0.021	0.339	0.047	
AT1G47 220	CYCA3.3	0.594	0.028	0.428	0.027	0.515	0.344	0.042	0.364	0.005	0.344
		0.598	0.025	0.440	0.024		0.332	0.008	0.334	0.025	
AT1G03120	RAB28	0.220	0.013	0.415	0.024	0.348	0.389	0.021	0.487	0.029	0.418
		0.298	0.032	0.458	0.031		0.376	0.024	0.421	0.021	
AT1G08160	late embryogenesis abundant (LEA) hydroxyproline-rich glycoprotein family	0.247	0.033	0.402	0.009	0.334	0.292	0.040	0.427	0.014	0.349
		0.247	0.036	0.440	0.008		0.229	0.034	0.449	0.035	
Hormone-Related											
AT5G56 650	IAA-amino acid hydrolase ILR1-like 1	0.747	0.016	0.713	0.038	0.748	0.259	0.023	0.255	0.004	0.238
		0.748	0.025	0.785	0.031		0.223	0.036	0.216	0.007	
AT1G77 850	auxin response factor 17	0.954	0.005	0.911	0.029	0.947	0.305	0.048	0.399	0.014	0.348
		0.925	0.009	0.996	0.021		0.358	0.032	0.328	0.021	
AT2G28 350	auxin response factor 10	0.218	0.036	0.411	0.019	0.319	0.337	0.007	0.483	0.015	0.402
		0.225	0.032	0.420	0.032		0.349	0.008	0.440	0.032	
AT2G46 370	encodes a jasmonate-amido synthetase that is a member of the GH3 family of proteins	1.776	0.005	1.724	0.002	1.708	2.106	0.039	2.238	0.044	2.197
		1.784	0.005	1.548	0.007		2.224	0.032	2.220	0.035	
AT1G02400	encodes a gibberellin 2-oxidase that acts on C19 gibberellins	0.556	0.038	0.596	0.006	0.558	0.573	0.005	0.597	0.006	0.548
		0.552	0.035	0.526	0.005		0.469	0.004	0.553	0.036	
AT1G15 550	gibberellin beta-hydroxylase 1	0.586	0.039	0.454	0.038	0.529	0.488	0.040	0.441	0.046	0.462
		0.524	0.038	0.552	0.032		0.472	0.007	0.448	0.039	
Transcriptional Factors											
AT1G68 130	transcriptional factor IDD14α	1.123	0.005	1.214	0.012	1.219	1.123	0.007	1.216	0.023	1.247
		1.216	0.021	1.321	0.016		1.221	0.015	1.425	0.022	
AT1G68 130	transcriptional factor IDD14β	0.497	0.021	0.364	0.025	0.423	0.404	0.016	0.368	0.043	0.382
		0.498	0.035	0.332	0.035		0.429	0.021	0.326	0.035	
AT1G32 330	heat shock transcription factor A1D	1.433	0.008	1.363	0.040	1.377	2.232	0.033	2.101	0.036	2.193
		1.442	0.009	1.269	0.035		2.220	0.036	2.220	0.035	
AT1G67 970	heat shock transcription factor A8	0.361	0.026	0.228	0.040	0.204	0.734	0.035	0.397	0.031	0.569
			0.021	0.226	0.024		0.724	0.025	0.421	0.038	
AT1G06850	basic leucine-zipper transcriptional factor 52	0.448	0.001	0.216	0.007	0.335	0.368	0.034	0.369	0.049	0.364
		0.459	0.008	0.215	0.008		0.319	0.008	0.401	0.047	
AT1G13 960	WRKY DNA-binding protein 4	0.881	0.044	0.183	0.035	0.519	1.867	0.022	1.879	0.035	1.820
		0.858	0.021	0.153	0.002		1.759	0.021	1.775	0.035	
AT1G55 600	WRKY DNA-binding protein 10	0.921	0.015	0.773	0.041	0.844	1.995	0.012	1.992	0.020	1.886
		0.956	0.032	0.725	0.025		1.779	0.021	1.776	0.008	
AT4G26 400	WRKY DNA-bind protein 34	2.234	0.010	2.137	0.036	2.212	1.117	0.008	1.112	0.000	1.165
		2.256	0.021	2.220	0.031		1.210	0.008	1.221	0.007	

dx.doi.org/10.1021/pr401262d | J. Proteome Res. 2014, 13, 2495−2510

Table 1. continued

accession number[a]	protein names	117:113[b]	p value	119:115[b]	p value	average degree	117:113[c]	p value	119:115[c]	p value	average degree
	Energy and Material Metabolism	118:114[b]	p value	121:116[b]	p value		118:114[c]	p value	121:116[c]	p value	
Transcriptional Factors											
AT1G08810	MYB domain protein 60	0.554	0.001	0.535	0.024	0.541	1.157	0.033	0.944	0.025	1.024
		0.552	0.009	0.524	0.003		1.128	0.032	0.868	0.012	
AT3G54 620	bZIP transcription factor-like protein mRNA	2.519	0.044	2.488	0.029	2.386	3.195	0.007	3.736	0.021	3.314
		2.214	0.021	2.321	0.005		3.102	0.007	3.221	0.037	

[a]TIAR number from www.arabidopsis.org. [b]Four differential individual iTRAQ experiments between *cbp20* and col-0 after 3 days of 100 mM salt stress; the tags of 117, 118, 119, and 121 were used to label the samples of *cbp20*, and the tags of 113, 114, 115, and 116 were used to label the samples of col-0. [c]Four differential individual iTRAQ experiments between *cbp80* and col-0 after 3 days of 100 mM salt stress; the tags of 117, 118, 119, and 121 were used to label the samples of *cbp80*, and the tags of 113, 114, 115, 116 were used to label the samples of col-0.

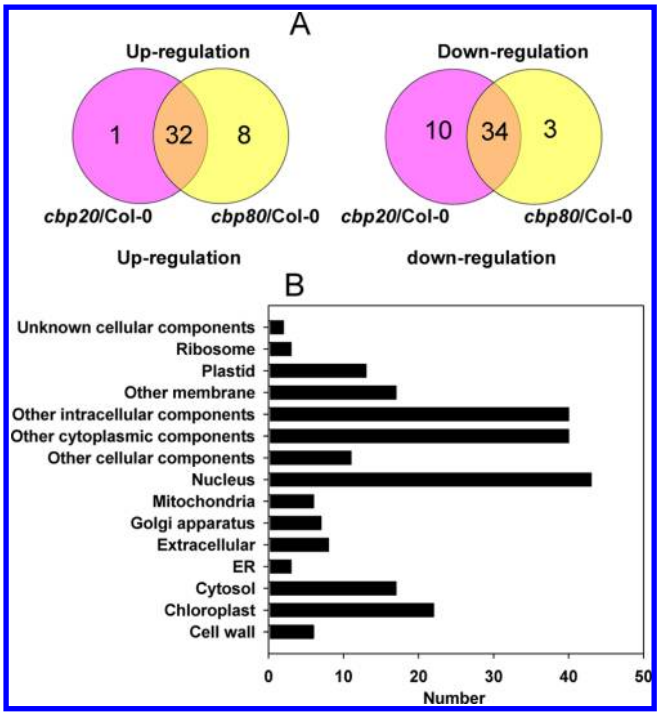

Figure 3. Characterization of the proteins differentially expression in the wild type, *cbp20*, and *cbp80* after exposure to salt stress. Differential expression (A) and GO analysis (B) of protein expression profiles in 2-week-old wild-type, *cbp20*, and *cbp80* seedlings in response to 3 days of salt stress treatment (100 mM NaCl).

amplified a band in *cbp20* and *cbp80*, indicating that the T-DNA insertion is indeed present in the *CBP20/CBP80* region (Figure 1B). Quantitative RT-PCR showed that the *cbp20* and *cbp80* lines had very low levels of *CBP20* and *CBP80* transcripts in comparison with the wild type Col-0 line. We also crossed the *cbp20* and *cbp80* lines to generate the *cbp20/80* double mutant. Similarly, T-DNA insertions were confirmed by PCR-based genotyping and qRT-PCR analysis (Figure 1B,C).

Localization of CBP20 and CBP80

We examined the localization of *CBP20* and *CBP80* in transgenic plants harboring GUS fusions of the *CBP20* or *CBP80* promoters. Analysis of GUS expression in *ProCBP20:-GUS* and *ProCBP80:GUS* transgenic lines showed that *CBP20* and *CBP80* were both constitutively expressed. *CBP20* and *CBP80* expression was strong in the seeds, leaves, flowers, and roots (Supplemental Figure 1A,B in the Supporting Information), suggesting that CBP20 and CBP80 have ubiquitous roles in plant growth and development, which correlates with previous study.[3]

To determine the localization of CBP20 and CBP80 proteins, we fused *CBP20* and *CBP80* to the GFP gene and expressed these constructs under the constitutively active cauliflower mosaic virus (CaMV) 35S promoter (named *Pro35S:CBP20-GFP* and *Pro35S:CBP80-GFP*, respectively). Then, we transiently expressed *Pro35S:CBP20-GFP* and *Pro35S:CBP80-GFP* in tobacco leaves by Agrobacterium-mediated injection or in *Arabidopsis* protoplasts. We observed strong GFP fluorescence in the nuclei of tobacco leaves (Supplemental Figure 2A,B in the Supporting Information) and *Arabidopsis* protoplasts (Supplemental Figure 2C,D in the Supporting Information), suggesting that CBP20 and CBP80 function in the nucleus. Such location also coincide with the

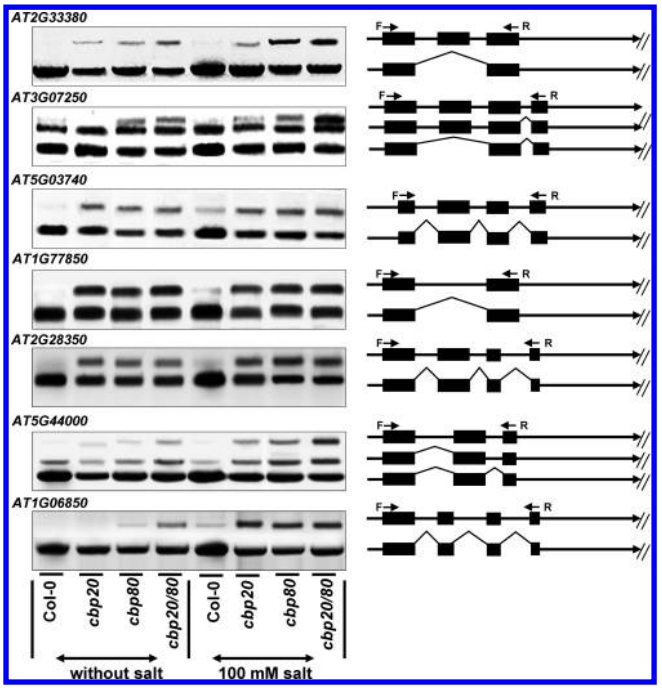

Figure 4. Alternative splicing of pre-mRNAs encoding proteins that were differentially expressed in *cbp20* and *cbp80* after salt stress compared with the wild type. The wild type, *cbp20*, *cbp80*, and *cbp20/80* were treated with or without 100 mM NaCl for 24 h, and the total RNA was extracted. The indicated genes were downregulated, as shown by RT-PCR using the corresponding primer pairs listed in Supplemental Table 2 in the Supporting Information. The alternatively spliced pre-mRNA products were isolated by agarose gel electrophoresis. The right panel indicates the genomic structure of these genes. Black boxes represent exons, lines indicate untranslated regions, and the arrows show PCR primers.

functions of CBP20 and CBP80 of regulating gene transcription and epigenetic regulation in the nucleus.

cbp20 and cbp80 Exhibit Increased Sensitivity to Salt Stress

Given that CBP20 and CBP80 are involved in ABA signal transduction and drought stress,[2,5] we wanted to investigate if they also function in salt stress. We thus examined their sensitivity to salt stress. When grown on vertical MS plates without salt stress, the root lengths of 2 week old *cbp20* seedlings were similar to those of the wild type, whereas *cbp80* and *cbp20/80* root growth was more severely inhibited under salt stress (Figure 2A). Exposure to an increasing gradient (25−100 mM) of salt (NaCl) resulted in a gradual reduction in root length of *cbp20*, *cbp80*, and *cbp20/80* plants. Furthermore, the *cbp20/80* double mutant was more sensitive to high concentrations of salt than was either of the single mutants (Figure 2A,B). Similarly, the *cbp20*, *cbp80*, and *cbp20/80* mutants were sensitive to salt stress when grown on soil irrigated with 100 mM salt (Figure 2C), and the salt-sensitive phenotype of *cbp20/80* was more pronounced than that of either of the single mutants. In addition, the biomass of 2 week old *cbp20*, *cbp80*, and *cbp20/80* plants grown in the salt-treated soil was lower than that of the wild type (Figure 2D).

Dynamic Protein Profiling of cbp20 and cbp80 Seedlings Subjected to Salt Stress

To establish the underlying function of CBP20 and CBP80 in the salt stress response, we conducted an iTRAQ (isobaric tags for relative and absolute quantitation) proteome analysis of differential protein changes in wild type, *cbp20*, and *cbp80* plants after 3 days of treatment with 100 mM NaCl. Total spectra were generated, and the data collected were analyzed using Mascot software. Using this approach, we identified 20

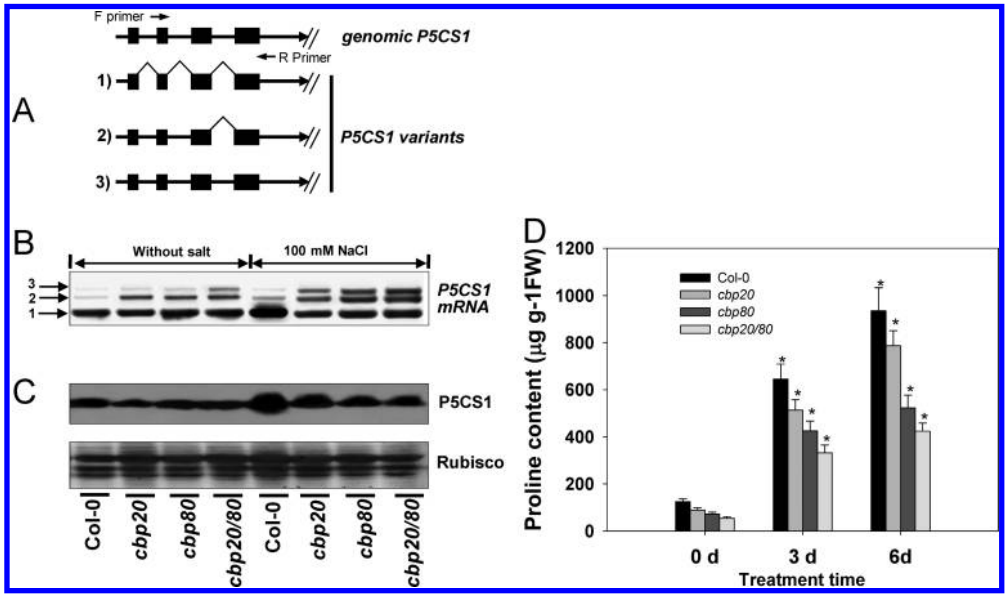

Figure 5. CBP20 and CBP80 modulate proline metabolism during the salt stress response in *Arabidopsis*. (A) Genomic structure of *P5CS1* and its alternatively spliced variants. Black boxes represent exons and lines indicate untranslated regions. PCR primers are labeled with arrows. (B,C) Alternative splicing of *P5CS1* pre-mRNA and its protein expression in the wild type, *cbp20*, *cbp80*, and *cbp20/80* treated or not with 100 mM NaCl for 24 h. The alternative splicing variants of *P5CS1* pre-mRNA were quantified by RT-PCR (B), or 2 week old plants were treated or not with 100 mM NaCl for 3 days and P5CS1 accumulation was measured using the anti-P5CS1 antibody (C). Ribulose-1,5-bisphosphate carboxylase/oxygenase (Rubisco) served as a loading control. (D) Difference in proline content in Col-0, *cbp20*, *cbp80*, and *cbp20/80* before and after 3 days of salt stress treatment (100 mM). Data are means ± SD (n = 12), and bars labeled with an asterisk are significantly different at $p < 0.05$ compared with the control experiments (Student's t test).

dx.doi.org/10.1021/pr4012624 | J. Proteome Res. 2014, 13, 2495−2510

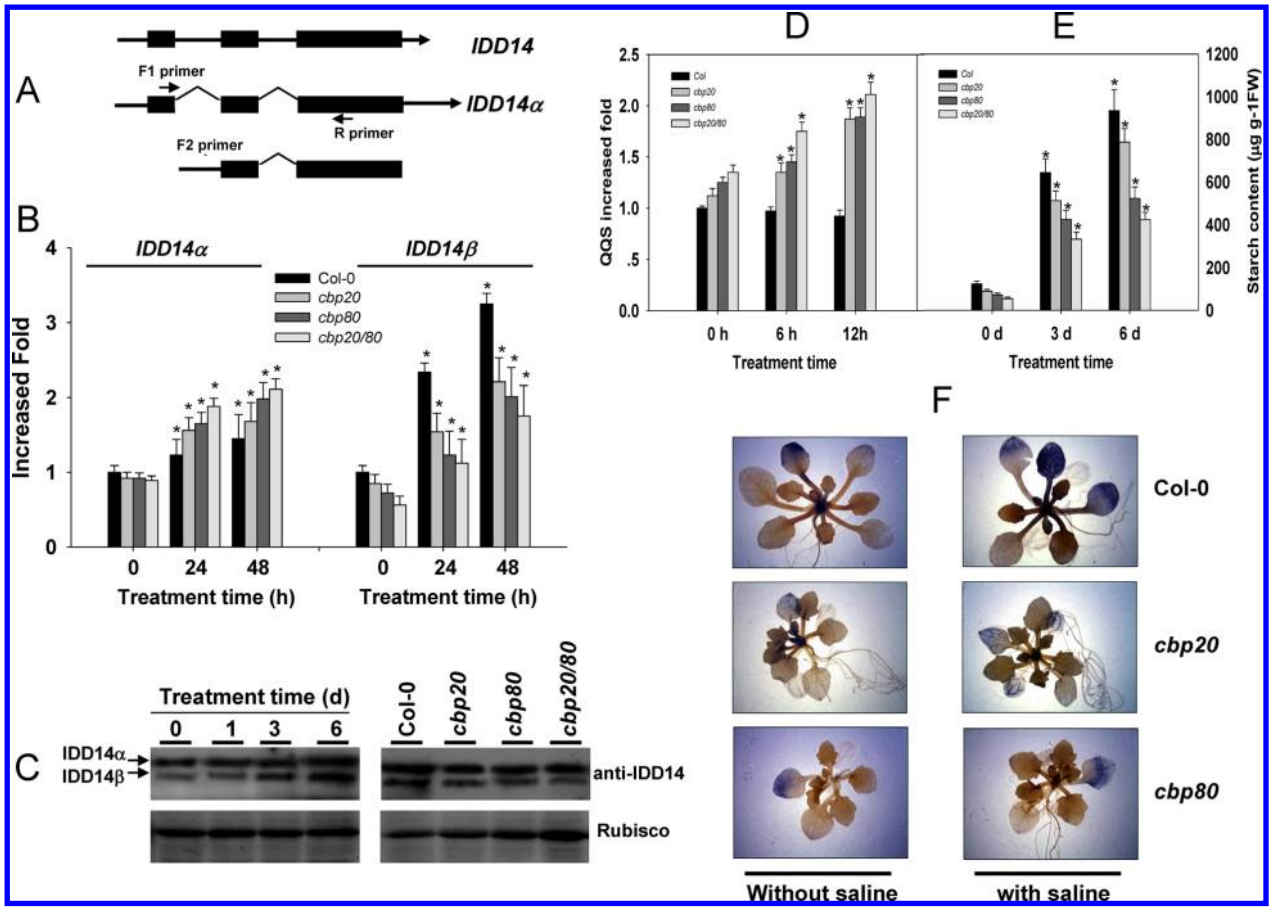

Figure 6. CBP20 and CBP80 modulate starch metabolism in *Arabidopsis* plants exposed to salt stress. (A) Genomic structure of *IDD14* and the structure of the alternatively spliced *IDD14α* and *IDD14β* mRNA variants. Black boxes represent exons and lines indicate untranslated regions. PCR primers are labeled with arrows. (B) Alternative splicing of *IDD14* pre-mRNA and its protein expression in wild-type, *cbp20*, *cbp80*, and *cbp20/80* lines exposed or not to 100 mM NaCl for 24 h, and the alternative splicing variants of *IDD14α* and *IDD14β* were measured by RT-PCR and the corresponding primer pairs. (C) Wild-type line was treated with 100 mM NaCl for the indicated period, and IDD14*α* and IDD14*β* protein accumulation was detected using anti-IDD14 antibody (left panel). The wild-type, *cbp20*, *cbp80*, and *cbp20/80* lines were treated with 100 mM NaCl for 3 days, and IDD14*α* and IDD14*β* proteins were detected using anti-IDD14 antibody (right panel). Ribulose-1,5-bisphosphate carboxylase/oxygenase (Rubisco) served as a loading control. (D) QQS gene expression in Col-0, *cbp20*, *cbp80*, and *cbp20/80* before and after 6 and 12 h of exposure to 100 mM NaCl. (E) Starch content in Col-0, *cbp20*, *cbp80*, and *cbp20/80* before and after 3 and 6 days of exposure to 100 mM NaCl. Data are the means ± SD (n = 12), and bars labeled with an asterisk are significantly different at $p < 0.05$ compared with the corresponding control (Student's t test). (F) Lugol solution staining indicated the starch content in Col-0, *cbp20*, and *cbp80* leaves with or without 3 days of saline treatment.

587 unique peptides and 3994 proteins. Over 67% of the proteins identified included at least two peptides.

We determined the ratios of protein abundance for the following four groups: (1) *cbp20* (control)/wild type (control), (2) *cbp80* (control)/wild type (control), (3) *cbp20* (salt stress)/wild type (salt), and (4) *cbp80* (salt)/wild type (salt) for proteins affected by salt stress in the *cbp20* and *cbp80* mutants. With a threshold of fold-change cutoff of >2-fold for increased expression and <0.6-fold for decreased expression, a total of 40 proteins differed significantly ($p < 0.05$) in the comparisons of WT, *cbp20*, and *cbp80* without NaCl treatment (control experiments, Supplemental Table 3 in the Supporting Information). Some of these 40 proteins were associated with auxin signaling, such as AT2G44080 (ARGOS-like protein), AT2G46370 (auxin-responsive GH3 family protein), and AT5G56650 (IAA-amino acid hydrolase ILR1-like 1), suggesting a mechanism whereby CBP20/80 mediates auxin distribution or leaf shape development. Furthermore, some proteins related to epigenetic modification or RNA biogenesis, including microRNA biosynthesis, such as AT3G54560 (histone H2A 11), AT3G06400 (chromatin-remodeling protein 11), AT1G58470 (RNA-binding protein 1), and AT1G10930 (ATP-dependent DNA helicase), were also shown to be differentially expressed in the *cbp20* or *cbp80* mutants compared with the wild type in the absence of salt stress. These data support previous findings that CBP20/CBP80 regulates microRNA biosynthesis to modulate leaf development.[3,4] Proteins involved in ubiquitination or SUMO modification, such as AT1G55860 (E3 ubiquitin-protein ligase UPL1), were also differentially expressed, suggesting that CBP20 and CBP80 are involved in post-transcriptional modification during plant growth and development.

Our iTRAQ results showed that a total of 77 proteins had significant differences in expression ($p < 0.05$, increased >2-fold or decreased <0.6-fold) in the *cbp20* or *cbp80* mutant compared with the wild type (Table 1, Supplemental Tables 4 and 5 in the Supporting Information). Among these 77 proteins, 33 and 40 were up-regulated in *cbp20* or *cbp80*, respectively, under salt stress compared with the wild type, and 44 and 37 proteins were down-regulated in *cbp20* and *cbp80*, respectively, under

dx.doi.org/10.1021/pr4012624 | J. Proteome Res. 2014, 13, 2495−2510

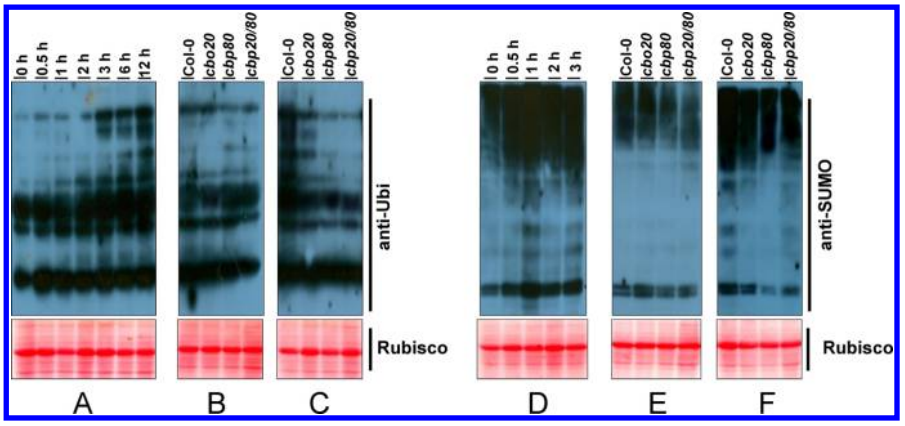

Figure 7. CBP20 and CBP80 modulate the protein ubiquitination and sumoylation status during the salt stress response. (A,D) Wild-type line was treated with 100 mM NaCl for the indicated periods, and protein ubiquitination and sumoylation status were measured using anti-UBI and anti-SUMO antibody, respectively. (B,C) Wild-type, *cbp20*, *cbp80*, and *cbp20/80* lines were treated with 100 mM NaCl for 1 (B) and 12 h (C), and the protein ubiquitination status was measured using anti-Ubi antibody. (E,F) Wild-type, *cbp20*, *cbp80*, and *cbp20/80* lines were treated with 100 mM NaCl for 1 (E) and 12 h (F), and the protein sumoylation status was measured using the anti-SUMO antibody. Ribulose-1,5-bisphosphate carboxylase/oxygenase (Rubisco) served as a loading control.

saline stress compared with the wild type (Figure 3A, Supplement Figure 3 in the Supporting Information). On the basis of Gene Ontology analysis (WEGO, http://wego.genomics.org.cn) and BLAST alignments, the proteins that exhibited significant changes under normal conditions and salt treatment were classified into eight functional categories, namely, energy and material metabolism, defense-response-related, ubiquitination and sumoylation modification, epigenetic modification, protein kinase and phosphatase, cell division and structure, hormone-related, and transcriptional factors (Figure 3B). In particular, proteins involved in epigenetic modification, such as AT1G10930 (ATP-dependent DAN helicase), At2g25170 (encodes an SWI/SWF nuclear-localized chromatin remodeling factor of the CHD3 group), AT3G54610 (encodes a histone acetyltransferase), and AT5G03740 (HD2-type histone eactylase HDAC); involved in ubiquitination and sumoylation modification, such as AT1G55860 (E3 ubiquitin ligase family protein), AT2G36060 (ubiquitin-conjugating enzyme E2 variant 1C), AT1G55860 (encodes a ubiquitin-protein ligase), AT3G48340 (cysteine proteinases superfamily protein), and AT5G05080 (ubiquitin-conjugating enzyme 22); and involved in defense responses, such as AT1G02920 (encodes glutathione transferase), AT4G18350 (encodes 9-*cis*-epoxycarotenoid dioxygenase), AT2G39800 (encodes a delta1-pyrroline-5-carboxylate synthase), and AT5G44000 (glutathione S-transferase family protein) were coincidentally up-regulated or down-regulated after salt stress in the *cbp20* and *cbp80* mutants, indicating that CBP20 and CBP80 coordinately modulate protein expression during the saline stress response (Table 1, Supplemental Figure 3 in the Supporting Information).

CBP20 and CBP80 Modulate pre-mRNA Alternative Splicing under Salt Stress

It is reported that CBP20 interacts with CBP80 to participate in pre-mRNA alternative splicing to modulate gene expression,[3,19] and thus it is possible that CBP80 functions coordinately with CBP20 to regulate differential protein accumulation by synergistically controlling the alternative splicing of genes under salt stress. To test this possibility, we examined the transcriptional products of several genes that encode proteins showing significant differential expression in our iTRAQ analysis (Figure 4). For instance, we examined the transcriptional products of *AT2G33380*, which encodes a calcium-binding protein and is induced by salt, ABA, and drought stress.[20] The encoded protein was markedly down-regulated in *cbp20* and *cbp80* compared with the wild type after exposure to salt stress. RT-PCR analysis of *cbp20* and *cbp80* seedlings using primers specific to *AT2G33380* revealed a prominent band and a slower moving minor band. Whereas the prominent band was also present in the wild type, the minor band was barely detectable. Further analysis using primers corresponding to the first and third exon confirmed that the larger band in the *cbp20* and *cbp80* mutants resulted from the retention of the first and second introns. Salt stress increased the accumulation of the smaller band in wild-type seedlings but increased the abundance of the larger band in *cbp20* and *cbp80*. The intensity of the larger band was greatest in the *cbp20/cbp80* double mutant, suggesting that CBP20 and CBP80 act synergistically to direct the correct splicing of this gene (Figure 4). This gene could be modulated by histone methylation, and CBP20 and CBP80 CBC may modify the corresponding histones.[21,22] Furthermore, *AT3G07250* and *AT5G03740* encode a putative RNA-binding protein and HD2-type histone deacetylase HDAC protein, respectively. These two proteins were down-regulated in *cbp20* and *cbp80* after exposure to saline stress compared with the wild type. RT-PCR of these two genes showed that a large minor band that was absent in the wild type appeared in the *cbp20* and *cbp80* mutants before saline stress and that the intensity of this band increased after salt stress, becoming visible in the wild-type sample (Figure 4). It is possible that the aberrant pre-mRNA splicing of these two genes in *cbp20* and *cbp80* caused the down-regulation of the proteins encoded by *AT3G07250* and *AT5G03740*. In line with this notion, these two proteins are involved in the response to abiotic stresses, such as ABA.[23] AUXIN RESPONSE FACTOR 10 (ARF10, AT2G28350) and AUXIN RESPONSE FACTOR 17 (ARF17, AT1G77850) are two important auxin-responsible proteins involved in plant development and environmental stress responses. We found that these two proteins were down-regulated in *cbp20* and *cbp80* mutants in the presence or absence of saline stress. In agreement with our iTRAQ data, RT-PCR analysis of these two genes showed one larger band in the *cbp20* and *cbp80* mutant that was absent in the wild type

dx.doi.org/10.1021/pr4012624 | *J. Proteome Res.* 2014, 13, 2495−2510

(Figure 4), suggesting that incorrect splicing of *ARF10* and *ARF17* resulted in the down-regulation of the two encoded proteins, which may underlie the abnormal serrations in the leaves of *cbp20* an *cbp80*. Because *ARF10* and *ARF17* are the targets of miR160[24,25] and ARF17 expression may be regulated by AGO1,[26] one component of the machinery that generates microRNA, it is possible that CBP20 and CBP80 affect the expression of *ARF10* and *ARF17* by regulating microRNA biogenesis. The reactive oxygen species burst and increase in antioxidant enzyme activity were characterized in plants subjected to abiotic stress, including saline stress.[6,27] We found that the antioxidant enzyme gene *AT5G44000*, which encodes a glutathione S-transferase family protein, exhibited incorrect splicing in the *cbp20* and *cbp80* mutants, and that salt stress increased the abundance of the incorrectly spliced band (Figure 4). This finding supports our iTRAQ data, which showed that the expression of both of these proteins was down-regulated in *cbp20* and *cbp80* before or after exposure to salt stress. These data indicate that CBP20 and CBP80 mediate many mechanisms during plant in response to saline stress, such as CBP20 and CBP80 mediating the gene splicing involved in the microRNA biogenesis (such as miR160 and its target genes *ARF10* and *ARF17*) and epigenetic regulators (such as RNA-binding protein and HDAC protein), the calcium signal (such as calcium-binding protein), or the redox status (such as antioxidant enzyme and its target metabolites, for example, hydrogen peroxide, superoxide ions, etc.). Similarly, the degree of aberrant splicing of *AT1G06850*, which encodes a basic leucine-zipper transcription factor (b-ZIP), was also increased in *cbp20* and *cbp80* after exposure to salt stress, and this effect was enhanced in the *cbp20/80* double mutant, suggesting the roles of CBP20/80-mediated splicing of transcriptional factors during saline stress.

CBP20- and CBP80-Dependent Alternative Splicing Modulates Proline Metabolism during Salt Stress

The amino acid proline accumulates in response to multiple forms of environmental stress, such as high temperature and cold.[17,28] Salt stress also increases proline content in *Arabidopsis*. *P5CS1* has a critical function in proline metabolism in plants. The alternative splicing of *P5CS1* in different ecotypes of *Arabidopsis* resulted in differential responses to osmotic stress.[29] Here we identified at least two types of *P5CS1* pre-mRNA splicing variants in the *cbp20* and *cbp80* mutants (Figure 5A,B). In addition, the abundance of the aberrant splicing products increased after exposure to salt stress (Figure 5B). This finding supported our iTRAQ data, which showed that the protein level of P5CS1 in the *cbp20* and *cbp80* mutants was at 0.394 and 0.270 times less than that in the wild type under saline stress (Table 1). We used an anti-P5CS1 antibody to monitor P5CS1 accumulation in the *cbp20*, *cbp80*, and *cbp20/80* mutants after exposure to salt stress. P5CS1 levels showed a marked increase in the wild type after exposure to salt stress; however, the increase was limited in *cbp20*, *cbp80*, and *cbp20/80* (Figure 5). Consistent with this finding, the proline content rapidly increased in the wild type after 3 or 6 days of salt stress, reacted about 0.8 and 1 mg g^{-1} FW. Whereas a similar increase in proline content was observed in *cbp20* and *cbp80* lines exposed to salt stress, the increase was markedly less than that in the wild type, only about half of wild type after saline stress. These data suggest that CBP20/80 mediates the correct splicing of *P5CS1* pre-mRNA, which is important for the salt stress-induced proline content increase and salt tolerance in *Arabidopsis*.

CBP20- and CBP80-Mediated IDD14 Splicing Modulates Starch Content during Salt Stress

Starch, as a source of carbon, is involved in the plant's response to environmental stress.[27,30] The transcription factor IDD14 binds to the promoter region of *Qua-Quine starch* (*QQS*), which regulates starch degradation, to modulate its expression.[18] Alternative gene splicing is involved in development and in stress responses.[31] *IDD14* has two different splicing variants; the larger variant is termed IDD14α, and the smaller variant, which lacks the first exon encoding the DNA-binding motif, is termed *IDD14*β (Figure 6A). The IDD14β form of protein can compete with IDD14α homodimers to generate IDD14α-IDD14β heterodimers, which reduce binding to the promoter of *QQS* and thereby reduce starch degradation.[18] In cold stress, the transcriptional increase in the IDD14b form reduced the ability of IDD14 to bind to the promoter region of *QQS* and thereby reduced *QQS* expression and prevented starch degradation.[18] Here we examined the alternative splicing of *IDD14* pre-mRNA using primers corresponding to the *IDD14*α and *IDD14*β form, respectively (Figure 6A). We found that one spectra corresponding to the first exon of *IDD14*α sustained high levels in the *cbp20* or *cbp80* mutant after salt stress, while the expression level of this spectra was markedly reduced in the wild type (Table 1, Supplemental Tables 1 and 2 in the Supporting Information), indicating that expression of the *IDD14*α form was higher in the *cbp20* and *cbp80* mutants than in the wild type. However, we noticed that the expression level of two other spectra, corresponding to the second and third exons, was increased in the wild-type lines (Table 1, Supplemental Tables 4 and 5 in the Supporting Information), suggesting that the IDD14β form was more abundant in the wild type after salt stress. These iTRAQ data suggest that differences in *IDD14*α and *IDD14*β expression were associated with the alternative splicing of *IDD14* during salt stress. To test this notion, we used RT-PCR analysis to determine the abundance of *IDD14*α and *IDD14*β transcripts in *cbp20*, *cbp80*, and wild-type plants under salt stress. The mRNA variant encoding the IDD14α type showed a marked increase in expression in the *cbp20* and *cbp80* mutants under salt stress compared with the wild type (Figure 6B). In contrast, the IDD14β type increased in the wild type under salt stress compared with *cbp20* and *cbp80*, which correlated with our iTRAQ data on the differential accumulation patterns of IDD14α and IDD14β in the *cbp20*, *cbp80*, and wild-type lines under salt stress. We also prepared a protein antibody corresponding to full-length IDD14. As shown in Figure 6C, this antibody detected two separate bands, representing the IDD14α and IDD14β forms, in the *cbp20*, *cbp80*, and wild-type lines in the absence of salt stress. The larger band, corresponding to the IDD14α form, did not show obvious changes in the *cbp20* and *cbp80* mutant after 3 days of salt stress, but the abundance of the smaller band, corresponding to the IDD14β form, gradually increased in the wild-type line but not in the *cbp20*, *cbp80*, and *cbp20/80* double mutant during salt stress treatment. Consistent with the expression pattern of IDD14α and IDD14β after salt stress, we found that *QQS* expression increased in the *cbp20* and *cbp80* lines, and to a greater extent in the double mutant, after salt stress, compared with the wild type (Figure 6D). The increase in the IDD14β form interfered with the binding of IDD14α to the promoter of

dx.doi.org/10.1021/pr4012624 | J. Proteome Res. 2014, 13, 2495−2510

QSS and thereby suppressed *QSS* transcription. It is possible that loss of CBP20 or CBP80 in the *cbp20* and *cbp80* mutant caused the incorrectly spliced variant of IDD14α to reduce the generation of IDD14β after exposure to salt stress, which caused an increase in the ratio of IDD14α to IDD14β, thus activating the transcription of *QQS* and causing increased starch degradation in *cbp20* and *cbp80*. In contrast, the increase in *IDD14β* accumulation in the wild type resulted in efficient splicing of *IDD14* and limited the binding of IDD14α to the promoter region of *QQS*, subsequently reducing *QQS* transcription. As a result, more starch accumulated in wild-type lines under salt stress, we found that the starch content in the wild type reached ~0.7 and 0.9 mg g^{-1} FW after 3 or 6 days of saline stress, while such content in the *cbp20* and *cbp80* was reduced by ~23% compared with wild type after saline stress (Figure 6E). The iodine solution staining can be used to visualize the starch accumulation in the plant. In agreement with the previously described transcriptional results, our staining results using Lugol solution (containing aqueous potassium iodide and iodine) staining indicated more starch accumulation in the leaves of wild type after saline stress, while less starch accumulation was observed in the *cbp20* or *cbp80* mutants after saline stress. Previous study demonstrates that salt stress induces starch accumulation, which improves the plant's defense response.[32] Here we also found that salt stress increased starch content in wild-type plants and that this was accompanied by an increase in *IDD14β* transcription and a reduction in *QQS* expression. It is possible that the sensitivity of *cbp20* and *cbp80* to salt stress results from the incorrect splicing of IDD14, which reduces IDD14β accumulation. As a result, *QQS* transcription is maintained at high levels, which promotes starch degradation and possibly underlies the sensitivity of *cbp20* and *cbp80* to salt stress.

Role of CBP20- and CBP80-Mediated Protein Ubiquitination and Sumoylation during Salt Stress

Protein sumoylation modification is associated with RNA-level epigenetic regulation,[33] and the CBC affects chromatin H2B ubiquitination by facilitating pre-mRNA splicing and histone H2B ubiquitination,[34] and is involved in chromatin epigenetic modification.[35] It is possible that CBP20 and CBP80 affect protein post-translation modification, such as ubiquitination or sumoylation modification. Our iTRAQ data showed that most ubiquitination- or sumoylation-related proteins, such as *AT2G36060*, which encodes ubiquitin-conjugating enzyme E2 variant 1C, and *AT5G60410*, which encodes a plant small ubiquitin-like modifier (SUMO) E3 ligase, were markedly up- and down-regulated, respectively, in the *cbp20* or *cbp80* mutant after salt stress compared with the wild-type line. It is possible that loss of CBP20 or CBP80 in the *cbp20* and *cbp80* mutants affects the degree of ubiquitination or sumoylation and thereby modulates the salt stress response. To test this possibility, we examined the degree of ubiquitination and sumoylation in the wild-type line after various periods of salt stress using specific antiubi and antisumo antibodies. As shown in Figure 7, salt stress induced a marked increase in protein ubiquitination and sumoylation in the wild type; however, the degree of ubiquitination and sumoylation in the *cbp20* and *cbp80* mutants was reduced after salt stress, and this reduction was likely related to the increased sensitivity of the mutants to salt stress. Miller et al. reported that several factors, such as STA1 (AT4G03430), regulate mRNA splicing as dynamic targets of stress-induced sumoylation in *Arabidopsis*.[33] For instance, STA1 interacts with CBP20/80 to mediate gene splicing or epigenetic modification,[36] and the CBC facilitates *SUS1* splicing by altering the H2B ubiquitination status.[34] These lines of evidence indicate the association between CBP20/80-mediated gene splicing and protein sumoylation/ubiquitination status. It is possible that CBP20/80 modulates gene splicing under salt stress by altering the protein ubiquitination and sumoylation status of key target components involved in gene splicing or epigenetic processes.

CONCLUSIONS

In this study, we successfully isolated the *cbp20* and *cbp80* mutants, both of which showed abnormal leaf and flower development and increased sensitivity to salt stress. To identify the underlying mechanisms whereby CBP20 and CBP80 modulate the response to salt stress in *Arabidopsis*, we performed a comparative iTRAQ analysis. We found that 77

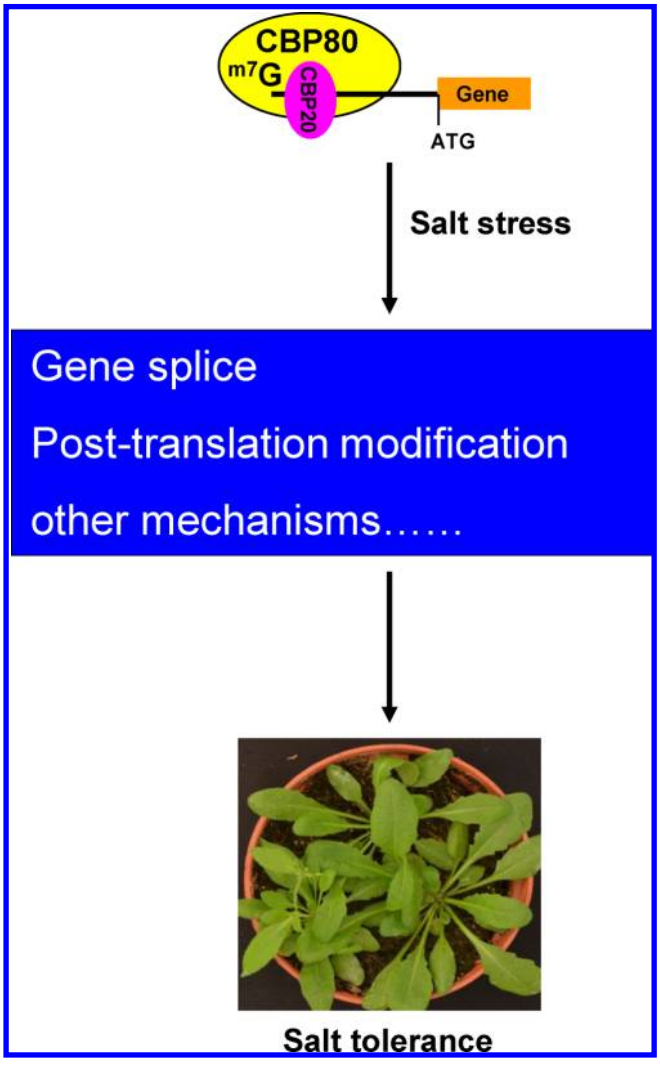

Figure 8. Schematic representation of a proposed model to explain the novel and synergistic mechanism by which CBP20 and CBP80 modulate the salt stress response in *Arabidopsis*. On the basis of our iTRAQ, genetic, and biochemical data, we propose that CBP20/80 mediates the alternative splicing of genes, such as *IDD14* and *P5CS1*, to control proline and starch levels, as well as protein ubiquitination and sumoylation, to modulate the salt stress response and microRNA biogenesis.

dx.doi.org/10.1021/pr4012624 | *J. Proteome Res.* 2014, 13, 2495−2510

proteins were differentially expressed (increased >2-fold or decreased <0.6-fold) in the mutants relative to the wild type. These proteins belonged to nine functional categories, including energy and material metabolism, defense-response-related, ubiquitination and sumoylation modification, epigenetic modification, protein kinase and phosphatase, cell division and structure, hormone-related, and transcriptional factors. The concentration of most of these proteins synergistically increased or decreased in *cbp20* or *cbp80* after salt stress, suggesting that CPB20 and CBP80 interact. As shown in Figure 8, we propose a model to illustrate the functions of CBP20 and CBP80 during plant in response to saline stress. Besides the reported roles of CBP20 and CBP80 in microRNA biogenesis during plant abiotic stress,[3,4] our biochemical experiments demonstrated that CBP20/80 mediated *P5CS1* and *IDD14* splicing to modulate P5CS1 and IDD14 protein expression and ultimately altered the proline and starch content to improve tolerance to salt stress. Furthermore, our results showed that CBP20/80 modulated the protein ubiquitination and sumoylation status of *Arabidopsis* in response to salt stress. Collectively, the quantitative data presented here reveal that CBP20 and CBP80 function in a coordinated fashion to modulate the salt stress response in *Arabidopsis*.

■ ASSOCIATED CONTENT

Supporting Information

Supplemental Figure 1 Subcellular localization of CBP20 and CBP80 protein in tobacco leaves and *Arabidopsis* protoplasts. Supplemental Figure 2 The ubiquitously expressions of CBP20 and CBP80 transcripts. Supplemental Figure 3: Hierarchical clustering for the differential expression protein profile among the *cbp20*, *cbp80*, and wild type Col-0 exposed to 100 mM saline stress. Supplemental Table 1: Labeling the proteins patterns for different treated samples by iTRAQ kit. Supplemental Table 2: The primer sequences used in this study. Supplemental Table 3: The differential expression ratios among 2-week-old wild-type (Col-0), *cbp20*, and *cbp80* seedlings not subjected to saline treatment. Supplemental Table 4: Identification of the differential proteins expression between 2-week-old *cbp20* mutant and wild-type (Col-0) seedlings subjected to 100 mM saline treatment. Supplemental Table 5: Identification of the differential proteins expression between 2-week-old *cbp80* mutant and wild type (Col-0) seedlings subjected to 100 mM saline treatment. This material is available free of charge via the Internet at http://pubs.acs.org.

■ AUTHOR INFORMATION

Corresponding Author

*E-mail: huxiangyang@mail.kib.ac.cn. Tel: 86-0871-65223069. Fax: 86-0871-65223398.

Notes

The authors declare no competing financial interest.

■ ACKNOWLEDGMENTS

We thank the ABRC for providing the seed stocks, Professor Jianmin Zhou (Institute of Genetics and Developmental Biology, Chinese Academy of Sciences) for the BRET vector, and Hao Yu (National University of Singapore) for the pOE-6HA vector. We also thank Dr. Kathleen Farquharson for careful reading and English polishing. This article was supported by the Major State Basic Research Development Program (2010CB951700), the Young Academic and Technical Leader Raising Foundation of Yunnan Province (No. 2012HB041), the National Science Foundation of China (No. 31170256), and the Natural Science Foundation of Jiangsu Province (No. BK2011409 to L.Y.).

■ REFERENCES

(1) Kuhn, J.; Hugouvieux, V.; Schroeder, J. mRNA Cap Binding Proteins: Effects on Abscisic Acid Signal Transduction, mRNA Processing, and Microarray Analyses. In *Nuclear pre-mRNA Processing in Plants*; Reddy, A. S. N., Golovkin, M., Eds.; Current Topics in Microbiology and Immunology *326*; Springer: Berlin, 2008; pp 139−150.

(2) Hugouvieux, V.; Kwak, J. M.; Schroeder, J. I. An mRNA Cap Binding Protein, ABH1, Modulates Early Abscisic Acid Signal Transduction in Arabidopsis. *Cell* **2001**, *106* (4), 477−487.

(3) Laubinger, S.; Sachsenberg, T.; Zeller, G.; Busch, W.; Lohmann, J. U.; Rätsch, G.; Weigel, D. Dual roles of the nuclear cap-binding complex and SERRATE in pre-mRNA splicing and microRNA processing in Arabidopsis thaliana. *Proc. Natl. Acad. Sci. U.S.A.* **2008**, *105* (25), 8795−8800.

(4) Kim, S.; Yang, J.-Y.; Xu, J.; Jang, I.-C.; Prigge, M. J.; Chua, N.-H. Two cap-binding proteins CBP20 and CBP80 are involved in processing primary microRNAs. *Plant Cell Physiol.* **2008**, *49* (11), 1634−1644.

(5) Papp, I.; Dulai, S.; Koncz, C. A mutation in the Cap Binding Protein 20 gene confers drought. *Plant Mol. Biol.* **2004**, *55* (5), 679−686.

(6) Zhu, J.-K. Plant salt tolerance. *Trends Plant Sci.* **2001**, *6* (2), 66−71.

(7) Barbazuk, W. B.; Fu, Y.; McGinnis, K. M. Genome-wide analyses of alternative splicing in plants: opportunities and challenges. *Genome Res.* **2008**, *18* (9), 1381−1392.

(8) Kornblihtt, A. R.; Schor, I. E.; Alló, M.; Dujardin, G.; Petrillo, E.; Muñoz, M. J. Alternative splicing: a pivotal step between eukaryotic transcription and translation. *Nat. Rev. Mol. Cell Biol.* **2013**, *14* (3), 153−165.

(9) Chinnusamy, V.; Zhu, J.-K. Epigenetic regulation of stress responses in plants. *Curr. Opin. Plant Biol.* **2009**, *12* (2), 133−139.

(10) Mazzucotelli, E.; Mastrangelo, A. M.; Crosatti, C.; Guerra, D.; Stanca, A. M.; Cattivelli, L. Abiotic stress response in plants: when post-transcriptional and post-translational regulations control transcription. *Plant Sci.* **2008**, *174* (4), 420−431.

(11) Nørregaard Jensen, O. Modification-specific proteomics: characterization of post-translational modifications by mass spectrometry. *Curr. Opin. Chem. Biol.* **2004**, *8* (1), 33−41.

(12) Mertins, P.; Qiao, J. W.; Patel, J.; Udeshi, N. D.; Clauser, K. R.; Mani, D.; Burgess, M. W.; Gillette, M. A.; Jaffe, J. D.; Carr, S. A. Integrated proteomic analysis of post-translational modifications by serial enrichment. *Nat. Methods* **2013**, *10*, 634−637.

(13) Yang, Y.; Chen, J.; Liu, Q.; Ben, C.; Todd, C. D.; Shi, J.; Yang, Y.; Hu, X. Comparative Proteomic Analysis of the Thermotolerant Plant Portulaca oleracea Acclimation to Combined High Temperature and Humidity Stress. *J. Proteome Res.* **2012**, *11* (7), 3605−3623.

(14) Bai, X.; Todd, C. D.; Desikan, R.; Yang, Y.; Hu, X. N-3-oxo-decanoyl-l-homoserine-lactone activates auxin-induced adventitious root formation via hydrogen peroxide-and nitric oxide-dependent cyclic GMP signaling in mung bean. *Plant Physiol.* **2012**, *158* (2), 725−736.

(15) Clough, S. J.; Bent, A. F. Floral dip: a simplified method for Agrobacterium-mediated transformation of Arabidopsis thalaian. *Plant J.* **1998**, *16* (6), 735−735.

(16) Wang, C.; Yin, X.; Kong, X.; Li, W.; Ma, L.; Sun, X.; Guan, Y.; Todd, C. D.; Yang, Y.; Hu, X. A Series of TA-Based and Zero-Background Vectors for Plant Functional Genomics. *PLoS One* **2013**, *8* (3), e59576.

(17) Zhao, M.-G.; Chen, L.; Zhang, L.-L.; Zhang, W.-H. Nitric reductase-dependent nitric oxide production is involved in cold

acclimation and freezing tolerance in *Arabidopsis*. *Plant Physiol.* **2009**, *151* (2), 755−767.
(18) Seo, P. J.; Kim, M. J.; Ryu, J.-Y.; Jeong, E.-Y.; Park, C.-M. Two splice variants of the IDD14 transcription factor competitively form nonfunctional heterodimers which may regulate starch metabolism. *Nat. Commun.* **2011**, *2*, 303 DOI: 10.1038/ncomms1303.
(19) Kierzkowski, D.; Kmieciak, M.; Piontek, P.; Wojtaszek, P.; Szweykowska-Kulinska, Z.; Jarmolowski, A. The Arabidopsis CBP20 targets the cap-binding complex to the nucleus, and is stabilized by CBP80. *Plant J.* **2009**, *59* (5), 814−825.
(20) Aubert, Y.; Vile, D.; Pervent, M.; Aldon, D.; Ranty, B.; Simonneau, T.; Vavasseur, A.; Galaud, J.-P. RD20, a stress-inducible caleosin, participates in stomatal control, transpiration and drought tolerance in Arabidopsis thaliana. *Plant Cell Physiol.* **2010**, *51* (12), 1975−1987.
(21) Deng, X.; Gu, L.; Liu, C.; Lu, T.; Lu, F.; Lu, Z.; Cui, P.; Pei, Y.; Wang, B.; Hu, S. Arginine methylation mediated by the Arabidopsis homolog of PRMT5 is essential for proper pre-mRNA splicing. *Proc. Natl. Acad. Sci. U.S.A.* **2010**, *107* (44), 19114−19119.
(22) Hossain, M. A.; Chung, C.; Pradhan, S. K.; Johnson, T. L. The yeast Cap Binding Complex modulates transcription factor recruitment and establishes proper histone H3K36 trimethylation during active transcription. *Mol. Cell. Biol.* **2013**, *33* (4), 785−799.
(23) Luo, M.; Wang, Y.-Y.; Liu, X.; Yang, S.; Lu, Q.; Cui, Y.; Wu, K. HD2C interacts with HDA6 and is involved in ABA and salt stress response in Arabidopsis. *J. Exp. Bot.* **2012**, *63* (8), 3297−3306.
(24) Wang, J.-W.; Wang, L.-J.; Mao, Y.-B.; Cai, W.-J.; Xue, H.-W.; Chen, X.-Y. Control of root cap formation by microRNA-targeted auxin response factors in Arabidopsis. *Plant Cell* **2005**, *17* (8), 2204−2216.
(25) Mallory, A. C.; Bartel, D. P.; Bartel, B. MicroRNA-directed regulation of Arabidopsis AUXIN RESPONSE FACTOR17 is essential for proper development and modulates expression of early auxin response genes. *Plant Cell* **2005**, *17* (5), 1360−1375.
(26) Sorin, C.; Bussell, J. D.; Camus, I.; Ljung, K.; Kowalczyk, M.; Geiss, G.; McKhann, H.; Garcion, C.; Vaucheret, H.; Sandberg, G. Auxin and light control of adventitious rooting in Arabidopsis require ARGONAUTE1. *Plant Cell* **2005**, *17* (5), 1343−1359.
(27) Vinocur, B.; Altman, A. Recent advances in engineering plant tolerance to abiotic stress: achievements and limitations. *Curr. Opin. Biotechnol.* **2005**, *16* (2), 123−132.
(28) Kishor, P. K.; Sangam, S.; Amrutha, R.; Laxmi, P. S.; Naidu, K.; Rao, K.; Rao, S.; Reddy, K.; Theriappan, P.; Sreenivasulu, N. Regulation of proline biosynthesis, degradation, uptake and transport in higher plants: its implications in plant growth and abiotic stress tolerance. *Curr. Sci.* **2005**, *88* (3), 424−438.
(29) Kesari, R.; Lasky, J. R.; Villamor, J. G.; Des Marais, D. L.; Chen, Y.-J. C.; Liu, T.-W.; Lin, W.; Juenger, T. E.; Verslues, P. E. Intron-mediated alternative splicing of Arabidopsis P5CS1 and its association with natural variation in proline and climate adaptation. *Proc. Natl. Acad. Sci. U. S. A.* **2012**, *109* (23), 9197−9202.
(30) Mittler, R. Abiotic stress, the field environment and stress combination. *Trends Plant Sci.* **2006**, *11* (1), 15−19.
(31) Seo, P. J.; Park, M.-J.; Park, C.-M. Alternative splicing of transcription factors in plant responses to low temperature stress: mechanisms and functions. *Planta* **2013**, *237* (6), 1415−1425.
(32) Pang, Q.; Chen, S.; Dai, S.; Chen, Y.; Wang, Y.; Yan, X. Comparative proteomics of salt tolerance in Arabidopsis thaliana and Thellungiella halophila. *J. Proteome Res.* **2010**, *9* (5), 2584−2599.
(33) Miller, M. J.; Scalf, M.; Rytz, T. C.; Hubler, S. L.; Smith, L. M.; Vierstra, R. D. Quantitative proteomics reveals factors regulating RNA biology as dynamic targets of stress-induced SUMOylation in Arabidopsis. *Mol. Cell. Proteomics* **2013**, *12* (2), 449−463.
(34) Hossain, M. A.; Claggett, J. M.; Nguyen, T.; Johnson, T. L. The cap binding complex influences H2B ubiquitination by facilitating splicing of the SUS1 pre-mRNA. *RNA* **2009**, *15* (8), 1515−1527.
(35) Luco, R. F.; Allo, M.; Schor, I. E.; Kornblihtt, A. R.; Misteli, T. Epigenetics in alternative pre-mRNA splicing. *Cell* **2011**, *144* (1), 16−26.
(36) Lee, B.-h.; Kapoor, A.; Zhu, J.; Zhu, J.-K. STABILIZED1, a stress-upregulated nuclear protein, is required for pre-mRNA splicing, mRNA turnover, and stress tolerance in Arabidopsis. *Plant Cell* **2006**, *18* (7), 1736−1749.